Biosensors and Bioelectronics 25 (2009) 901–905

Contents lists available at ScienceDirect

Biosensors and Bioelectronics

journal homepage: www.elsevier.com/locate/bios

Glucose Oxidase–graphene–chitosan modified electrode for direct electrochemistry and glucose sensing

Xinhuang Kang[a,b], Jun Wang[a], Hong Wu[a], Ilhan A. Aksay[c], Jun Liu[a], Yuehe Lin[a,*]

[a] Pacific Northwest National Laboratory, Richland, WA 99352, USA
[b] College of Science, Guangdong Ocean University, Guangdong, Zhanjiang 524088, PR China
[c] Department of Chemical Engineering, Princeton University, Princeton, NJ 08544, USA

ARTICLE INFO

Article history:
Received 2 July 2009
Received in revised form 27 August 2009
Accepted 1 September 2009
Available online 6 September 2009

Keywords:
Graphene
Glucose oxidase
Direct electron transfer
Chitosan

ABSTRACT

Direct electrochemistry of a glucose oxidase (GOD)–graphene–chitosan nanocomposite was studied. The immobilized enzyme retains its bioactivity, exhibits a surface confined, reversible two-proton and two-electron transfer reaction, and has good stability, activity and a fast heterogeneous electron transfer rate with the rate constant (k_s) of 2.83 s^{-1}. A much higher enzyme loading (1.12×10^{-9} mol/cm^2) is obtained as compared to the bare glass carbon surface. This GOD–graphene–chitosan nanocomposite film can be used for sensitive detection of glucose. The biosensor exhibits a wider linearity range from 0.08 mM to 12 mM glucose with a detection limit of 0.02 mM and much higher sensitivity (37.93 μA mM^{-1} cm^{-2}) as compared with other nanostructured supports. The excellent performance of the biosensor is attributed to large surface-to-volume ratio and high conductivity of graphene, and good biocompatibility of chitosan, which enhances the enzyme absorption and promotes direct electron transfer between redox enzymes and the surface of electrodes.

1. Introduction

Electron transfer in biological systems is a very important phenomenon for the areas of biochemical and biophysical sciences. Direct electron transfer (DET) between redox enzymes and the surface of electrodes can be used to investigate the enzyme-catalyzed reactions in biological systems and to lay the electrochemical basis for the study of the structure of enzymes, kinetics and thermodynamics of redox transformations of enzyme molecules, and metabolic processes involving redox transformations (Gooding et al., 2003; Pulcu et al., 2007; Wang et al., 2002). Great effort has been made to develop new mediator-free (or reagentless) biosensors, enzymatic bioreactors, and biomedical devices based on DET by immobilizing enzymes on conducting substrates (Guiseppi-Elie et al., 2002; Nadzhafova et al., 2007). However, the redox center in biomolecules is usually embedded deeply into the large three-dimensional structure of enzyme molecules (Andreu et al., 2007; Zhao et al., 2008a). Controlling the interactions of enzymes with the substrate to optimize the electron transfer processes remains a challenge. Many methods and materials, including biopolymers (Zhao et al., 2008a; Zhou et al., 2008; Shan et al., 2007), nanostructures (Jia et al., 2002; Liu et al., 2007; Luo et al., 2006; Nadzhafova et al., 2007) and sol–gel matrices (Jia et al., 2002; Zhang et al., 2007), have been studied to immobilize enzymes and promote electron transfer of redox enzymes on the surface of electrodes.

Recently, a new class of large surface-to-volume ratio, high conductivity carbon material, graphene, has attracted increasing attention for optoelectronic devices (Wang et al., 2008), supercapacitors (Vivekchand et al., 2008), gas sensors (Ao et al., 2008; Leenaerts et al., 2008; Schedin et al., 2007), pH sensor (Ang et al., 2008), chemical sensor (Wang et al., 2009a,b), biosensor (Shan et al., 2009) and nanocomposite (Li et al., 2008; Stankovich et al., 2006; Xu et al., 2008a,b) applications. Graphene is made of monolayers of two-dimensional honeycomb graphite type carbon (Geim and Novoselov, 2007; Novoselov et al., 2004). This unique nanostructure material has high surface area, excellent electrical conductivity and electron mobility at room temperature, robust mechanical properties, and flexibility (Stankovich et al., 2006). The special properties of graphene may provide insight to fabricate novel biosensors for virtual applications. The high surface area is helpful in increasing the surface loading of the target enzyme molecules on the surface. The excellent conductivity and small band gap are favorable for conducting electrons from the biomolecules (Stankovich et al., 2006). Graphene-based chemical sensors can also have a much higher sensitivity because of the low electronic noise from thermal effect (Ao et al., 2008; Peres et al., 2006). Furthermore, compared with CNTs, graphene can be obtained easily by chemical conversion of the inexpensive graphite (Xu et al., 2008a).

The successful dispersion of graphene has enabled the construction of various potentially useful graphene-based biosensors.

* Corresponding author. Tel.: +1 509 371 6227; fax: +1 509 371 6498.
E-mail address: yuehe.lin@pnl.gov (Y. Lin).

0956-5663/$ – see front matter © 2009 Elsevier B.V. All rights reserved.
doi:10.1016/j.bios.2009.09.004

Chemically functionalized graphene can be readily mixed with polymers in solution to form a stable dispersion and yield novel types of electrically conductive nanocomposites (Li and Kaner, 2008; Niyogi et al., 2006; Stankovich et al., 2006; Schniepp et al., 2006; Xu et al., 2008b). Graphene-based polymer nanocomposites display extraordinarily small electrical percolation threshold due to large conductivity and aspect ratio of the graphene sheets (Eda and Chhowalla, 2009; Liu et al., 2008a). Chitosan, a natural-biopolymer with unique structure features, possesses the primary amine at the C-2 position of the glucosamine residues and is soluble in aqueous acidic media at pH < 6.5. When dissolved and carried with the positive charge of $-NH_3^+$ groups, the chitosan can adhere to negatively charged surfaces or adsorb negatively charged materials. It is commonly used to disperse nanomaterials and immobilize enzymes for constructing biosensors due to its excellent capability for film formation, nontoxicity, biocompatibility, mechanical strength, and good water permeability. Chitosan can provide a good biocompatible microenvironment for proteins or enzyme (Kang et al., 2007; Yi et al., 2005; Zhang et al., 2004).

In this paper, the hybrid nanocomposite of graphene–chitosan was prepared and modified on the surface of glassy carbon electrode (GCE), and then GOD was absorbed on the nanocomposite film. The film was characterized with scanning electron microscopy and electrochemical methods. It was found that the nanocomposite film can provide a favorable microenvironment for GOD to realize DET. The GOD–Graphene–chitosan nanocomposite film can be used for glucose sensing and exhibit great sensitivity as compared with widely investigated carbon nanotubes-based ones. It opens up a new avenue for fabricating excellent electrochemical biosensors.

2. Experimental

2.1. Reagents and apparatus

Phosphate buffer saline (PBS 0.05 M, pH 7.4) with 0.1 M KCl was used as the supporting electrolyte. Natural flake graphite, sized at 45 μm, was kindly provided by Asbury Carbons (Asbury, NJ). Sulfuric acid (95%), potassium chlorate (98%), hydrochloric acid (37%), GOD (EC 1.1.3.4, Type X-S, 40,300 U/g), D-glucose, and chitosan were purchased from Sigma–Aldrich. The stock GOD solution was prepared in the PBS buffer and stored at 4 °C. A stock solution of D-glucose (0.1 M) was prepared and allowed to mutarotate at room temperature for 24 h before measurements. All other chemicals and reagents are of analytical grade and were prepared using ultrapure water (18.3 MΩ cm, Nanopure, Barnstead, USA).

The electrochemical experiments were performed with a CHI660a electrochemical workstation (CHI, Austin, TX). All experiments were carried out with a three-electrode system with a GCE (Φ = 3 mm) as the working electrode, a platinum wire as the auxiliary electrode, and an Ag/AgCl/3.0 M KCl as the reference electrode. Electrochemical impedance measurements were performed in a 0.1 M KCl solution containing 2 mM $K_3[Fe(CN)_6]$ + 2 mM $K_4[Fe(CN)_6]$ (1:1) and the results were plotted in the form of complex plane diagrams (Nyquist plots) with a frequency range from 0.1 Hz to 10 kHz. The amplitude of the applied sine wave potential is 5 mV, whereas the formal potential of the system was set at 0.23 V. The CV experiments were carried out in a quiescent solution at 100 mV s^{-1} in an electrochemical cell filled with 5.0 mL of PBS. LEO-982 scanning electron microscopy (SEM, Germany) was applied for characterizing the prepared samples.

2.2. Preparation of the graphene

The graphene was prepared according to the method (McAllister et al., 2007; Schniepp et al., 2006). Briefly, natural flake graphite was reacted with concentrated sulfuric acid and nitric acid with potassium chlorate for 96 h. After oxidation of graphite, the mixture was added to excess water, washed with a 5% solution of HCl, and then repeatedly washed with water until the pH of filtrate was neutral. Then through extremely rapid heating and successful splitting of graphite oxide, wrinkled graphene sheets functionalized with hydroxyl and carboxylic groups were obtained.

2.3. Fabrication of the GOD–graphene–chitosan film modified GCE

The GCE was polished with 1.0 μm, 0.3 μm, and 0.05 μm α-alumina powders and rinsed thoroughly with deionized water between each polishing step and sequentially sonicated in 1:1 HNO_3, ethanol, and deionized water, and dried at room temperature. Graphene (1 mg) was dispersed in 1 mL of 0.5 wt.% chitosan solution with ultra-sonication. Six microliters of the suspension was dropped on the surface of GCE and dried in air. Five microliters of GOD solution (10 mg/mL) was then coated on the graphene–chitosan film modified GCE (GOD–graphene–chitosan/GCE) and dried at 4 °C. Finally, the modified GCE was immersed in PBS to remove the loosely adsorbed GOD and was stored at 4 °C in a refrigerator under dry conditions when not in use.

3. Results and discussion

3.1. Dispersion of graphene by chitosan

When used as nanofiller into the chitosan matrix, similar to other polymers (Schniepp et al., 2006; Stankovich et al., 2006), graphene sheets may be performed for outstanding thermal, mechanical, and electrical properties. Here, a suspension containing graphene and chitosan was sonicated over 1 h. The graphene is well dispersed in the aqueous chitosan solution, forming a stable and dark suspension with only a small amount of graphene precipitated after 24 h. Fig. 1 is a SEM image of the graphene–chitosan composite deposited on the GCE surface, revealing the typical crumpled and wrinkled graphene sheet structure on the rough surface of the film. The results indicated that the edge plane of graphene sheets yielded chemical functional groups, such as C–OH and –COOH (Schniepp et al., 2006), in the thermal exfoliation process, which let graphene sheets are more hydrophilic and easier

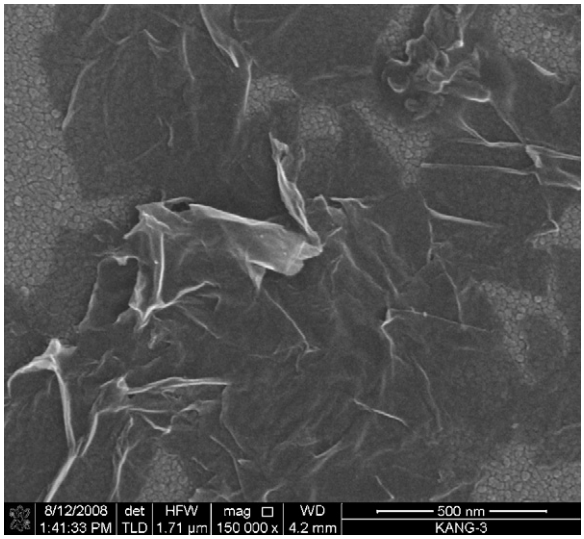

Fig. 1. SEM image of graphene–chitosan composite.

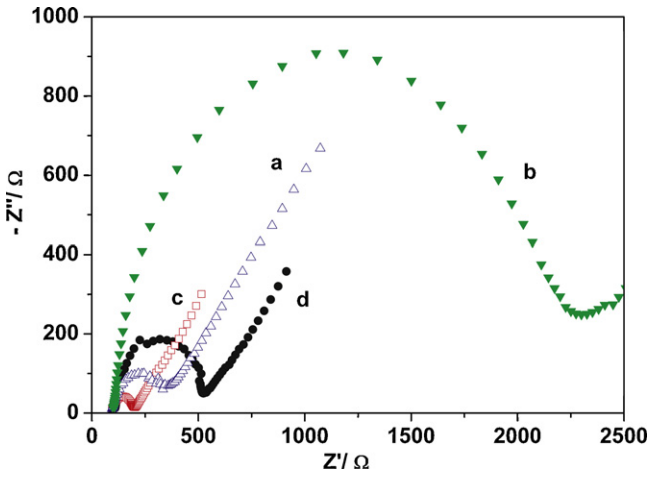

Fig. 2. Nyquist plot of EIS for (a–d) bare GCE, chitosan/GCE, graphene–chitosan GCE, and GOD–graphene–chitosan GCE.

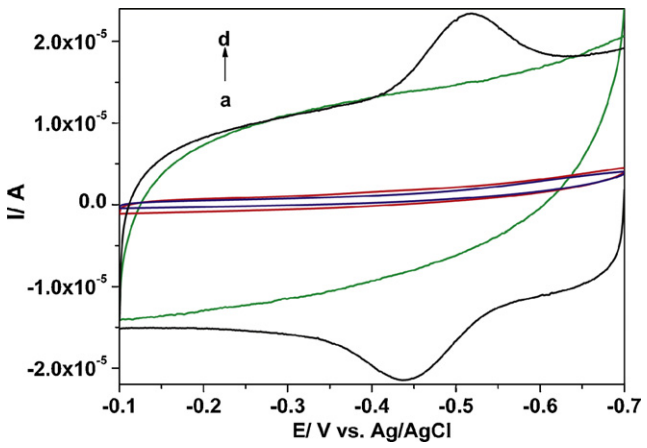

Fig. 3. Cyclic voltammograms of the modified GCEs with (a–d) chitosan, GOD-chitosan, graphene-chitosan, and GOD–graphene–chitosan films in PBS with N_2-saturated at the scan rate of 100 mV s^{-1}.

to interact with chitosan, facilitating the preparation of graphene-polymer composites (Stankovich et al., 2006).

3.2. Electrochemical impedance spectroscopy (EIS)

The electronic transfer properties of the electrode after different surface modifications were characterized by EIS (Ehret et al., 1997). The Nyquist plot of impedance spectra includes a semicircle portion and a linear portion. The semicircle portion at higher frequencies corresponds to the electron transfer limited process, and the linear portion at lower frequencies corresponds to the diffusion process. The electron transfer resistance (R_{ct}) at the electrode surface can be quantified using the diameter of the semicircle diameter. Fig. 2 shows the EIS diagrams of the bare and modified GCEs. The R_{ct} (2250 Ω, Fig. 2b) of the chitosan/GCE was much larger than that of the bare GCE (375 Ω, Fig. 2a), suggesting that a layer of chitosan could form on the electrode surface, and hinder the electron transfer from the redox probe of $[Fe(CN)_6]^{3-/4-}$, to the electrode surface. For the chitosan modified graphene on GCE (Fig. 2c), the R_{ct} drastically decreased to 210 Ω. Compared with chitosan or even the bare GCE surface, the graphene–chitosan film greatly improves the conductivity and the electron transfer process. When GOD is absorbed into the graphene–chitosan film, the R_{ct} would increase slightly to 505 Ω (Fig. 2d). This result indicated that the GOD was steadily adsorbed into the graphene–chitosan film, causing a little bit of inhibition of the electron transfer of the redox couple.

3.3. Direct electrochemistry of GOD immobilized in the graphene–chitosan film

FAD, a part of the GOD molecule, is known to undergo a redox reaction where two protons and two electrons are exchanged (Ianniello et al., 1982; Liu and Ju, 2003). Ianniello et al. (1982) suggested that the electrochemistry response of GOD immobilized on the solid surface is due to the redox reaction of FAD. Under appropriate conditions, direct electron transfer between GOD and the substrate can be observed from the electrochemical response and be used to prepare bioelectrocatalytic sensing devices (Deng et al., 2008; Guiseppi-Elie et al., 2002; Liu and Ju, 2003; Nadzhafova et al., 2007; Shan et al., 2009). Fig. 3 shows the cyclic voltammograms of GCEs coated with different films in N_2-saturated PBS at a scan rate 0.1 V s^{-1}. No peaks are observed for chitosan/GCE, GOD–chitosan/GCE, and graphene–chitosan/GCE (Fig. 3a–c). The background current of graphene–chitosan/GCE is higher than that of the chitosan/GCE, which is ascribed to the large surface area of the graphene–chitosan film. However, GOD on the surface of graphene–chitosan modified GCE shows distinct electrochemical response. Fig. 3d shows one pair of waves with anodic peak potential (E_{pa}) at −0.437 V and cathodic peak potential (E_{pc}) at −0.517 V. The peak potential separation (ΔE_p) is about 80 mV. The well-defined and quasi-reversible redox peaks suggest favorable direct electron transfer between the electrode and the redox centers of GOD molecules. Furthermore, the formal potential ($E^{0\prime}$) obtained by averaging potential values of the E_{pa} and E_{pc}, is −0.477 V. This value is close to the standard electrode potential of −0.505(vs. Ag/AgCl) for FAD/$FADH_2$ at pH 7.0 (25.8 °C) (Dai et al., 2007), suggesting that the GOD molecules retain its bioactivity after the adsorption on a graphene sheet

The influence of the scan rate on the cyclic voltammetric performance of the GOD–graphene–chitosan/GCE is investigated (Fig. 4). The redox processes of the GOD–graphene–chitosan nanocomposite gave roughly symmetric anodic and cathodic peaks at relatively slow scan rates. When the scan rate increases, the redox potentials (E_{pa} and E_{pc}) of GOD shift slightly. The ΔE_p, also increases, ranging from 0.02 V s^{-1} to 0.3 V s^{-1}. At the same time, the redox peak current increases linearly (inset, Fig. 4a; linear regression equations: $I_{pa} = 3.653 + 0.042\nu$, $r = 9988$; $I_{pc} = -1.697 - 0.049\nu$, $r = 0.9978$), in accordance with the equation: $i_p = nFQ\nu/4RT$ (Wen et al., 2007). Integration of the area under the reduction peaks gave nearly constant charge (Q) values independent of scan rate. All these characteristics suggest that the redox reaction of GOD on the graphene–chitosan film modified electrode is a quasi-reversible surface-controlled electrochemical process (Shan et al., 2009; Zhao et al., 2008a).

The electron-transfer-rate constant (k_s) of the GOD in the modified film can be estimated using the Laviron's model (Laviron, 1979). Plots of the E_{pa} and E_{pc} vs. the logarithm of the scan rates produce two straight lines with slops of $2.3RT/(1-\alpha)nF$ and $-2.3RT/\alpha nF$ (Zhao et al., 2008b) at high scan rates (Fig. 4b). From the slopes, α is estimated to be 0.54. The k_s of the GOD was calculated to be about $2.83 \pm 0.18\ s^{-1}$. This k_s is higher than those reported previously on MWCNTs paper (1.7 s^{-1}) (Guiseppi-Elie et al., 2002), on MWCNTs-chitosan (1.08 s^{-1}) (Luo et al., 2006), on boron-doped MWCNTs (1.56 s^{-1}) (Deng et al., 2008), and on MWCNTs-CTAB (1.53 s^{-1}) (Cai and Chen, 2004) modified electrodes, but close to that of GOD at SWCNTs-chitosan modified electrode (3.0 s^{-1}) (Zhou et al., 2008) and CNTs-poly(diallyldimethylammonium chloride) (PDDA) modified electrode (2.76 s^{-1}) (Wen et al., 2007). These results suggest that the graphene–chitosan modified electrode provides fast elec-

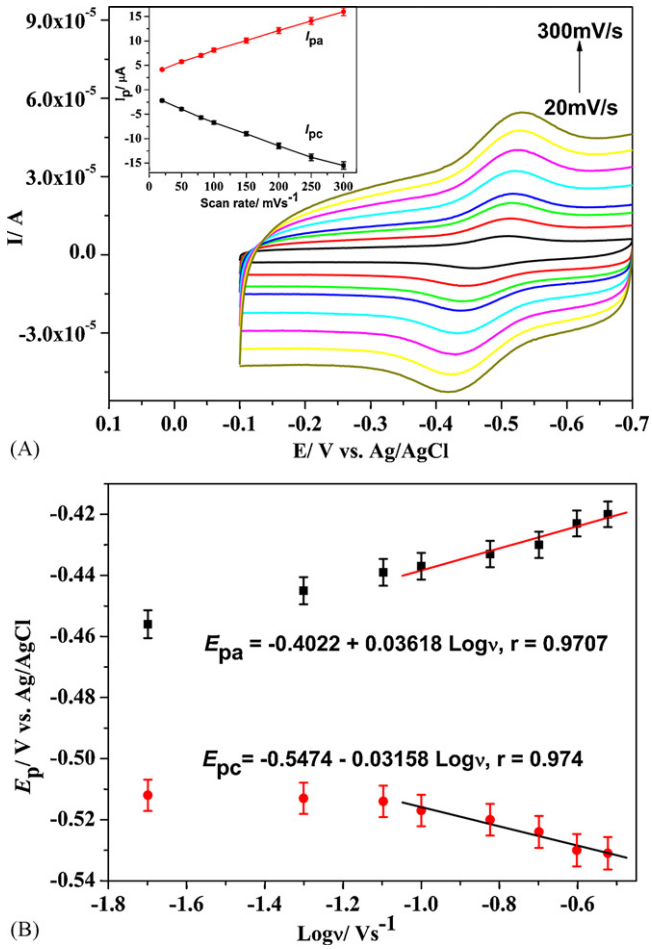

Fig. 4. Cyclic voltammograms of the modified GCE with GOD–graphene–chitosan film in PBS with 0.1 M KCl at different scan rates: 20, 50, 80, 100, 150, 200, 250, and 300 mVs^{-1} (a); the plot of the peak current vs. scan rates (a inset); and the relationship of the peak potential (E_p) vs. the logarithm of scan rate ($\log \nu$), the linear fitting at scan rates from 100 mVs^{-1} to 300 mVs^{-1} (b).

tron transfer between the redox center of the enzyme and the surface of electrode.

The surface average concentration of electroactive GOD (Γ moL/cm^2) on the film can be calculated from the charge integration of the cathodic peak in the cyclic voltammogram according to the formula, $Q = nFA\Gamma$, where Q is the charge consumed in C, A is the electrode area (cm^2), F is the Faraday constant, and n is the number of electrons transferred. The electroactive GOD concentration on the graphene–chitosan nanocomposite is estimated to be 1.12×10^{-9} mol/cm^2 ($n = 2$), which is three orders of magnitude higher than that (2.86×10^{-12} mol/cm^2) at the bare GCE (Liu and Ju, 2003), indicating saturated adsorption of GOD in multi-layers of the graphene nanocomposite film.

On the other hand, it is well known that the DET of GOD is a two-electron along with two-proton reaction that undergoes a redox reaction as follows (Liu and Ju, 2003):

$$\text{GOD-FAD} + 2e^- + 2H^+ \leftrightarrow \text{GOD-FADH}_2 \quad (1)$$

Therefore, the pH value of the solution should have an effect on the electrochemical behavior of GOD on the graphene–chitosan film. As shown in Fig. 5, a negative shift of both the cathodic and anodic peak potentials occurs when the solution pH value is increased. The redox potential $E^{0\prime}$ changes linearly as a function of solution pH from 6.54 to 9.87 with a slope of −61 mV/pH ($r = 0.9989$). This slope is close to the theoretical value of −58.6 mV/pH according to the reaction Eq. (1) (Liu et al., 2007) for

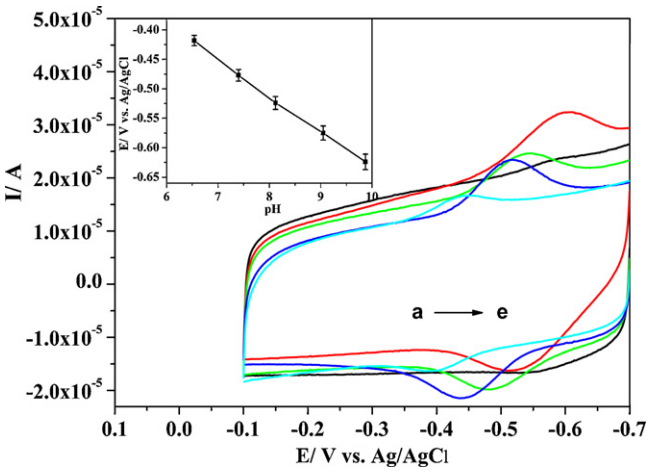

Fig. 5. Cyclic voltammograms of the modified GCE in PBS buffer solution with different pH values of (a–e) 6.54, 7.4, 8.12, 9.05, and 9.87; scan rate 100 mVs^{-1}; inset is the plot of formal potentials vs. pH.

a reversible, indicating two protons and two electrons attending in the electron transfer process.

The direct electron transfer of GOD is stable. The cyclic voltammetric responses of the GOD–graphene–chitosan modified electrode in N_2-saturated PBS (pH 7.4) show no obvious changes after 15 cycles, and then it decreases slowly with the increase in the cycles (data not shown here). The storage stability of the GOD–graphene–chitosan modified GCE was investigated. The cathodic peak current was measured using the same electrode and it retained above 95% of its initial response stored at 4 °C after 1 week. These results display that the direct electrochemistry of GOD immobilized on the surface of graphene–chitosan has a good stability and reproducibility.

3.4. Performance of the GOD–graphene–chitosan film-based glucose biosensor

Fig. 6 shows the CVs of the GOD–graphene–chitosan nanocomposite on the electrode in a solution containing different concentrations of glucose under the condition of Oxygen saturation. It can be seen from this figure that the baseline of the reduction decreased with the increase in glucose concentration indicating the oxygen consumption. It was found that the oxygen consumption is

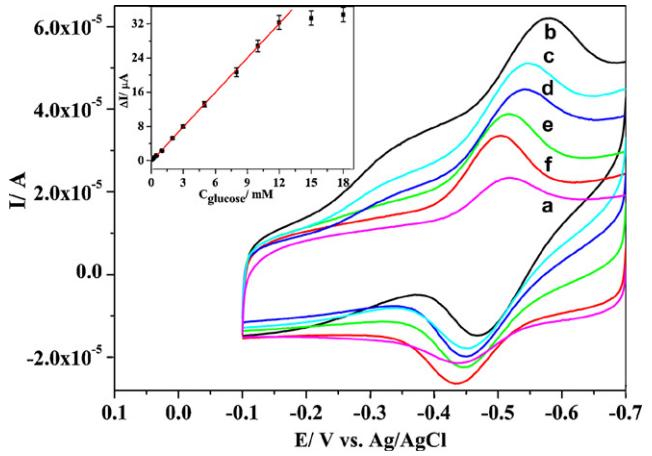

Fig. 6. Cyclic voltammograms of GOD–graphene–chitosan/GCE in PBS with 0.1 M KCl at a scan rate of 100 mVs^{-1} in the presence of different concentrations of glucose (a) N_2-saturated without glucose, (b) O_2-saturated without glucose, and (c–f) with glucose of 3.0, 5.0, 8.0, and 10.0 mM.

linearly increased with the increase in glucose concentration ranging from 0.08 mM to 12 mM with a correlation coefficient (R) of 0.9993 and a high sensitivity of about 37.93 $\mu A\,mM^{-1}\,cm^{-2}$ (Fig. 6 inset). Therefore, this GOD–graphene–chitosan nanocomposite can be served as a glucose sensor. It is well known that the diabetic glucose concentration is above 7.0 mM (Dai et al., 2007), which indicates that this biosensor is suitable for its practical application for the determination of human blood sugar concentration. This linear range is much wider than that of 0–7.8 mM for GOD on the MWCNTs-chitosan matrix (Liu et al., 2005), 0.08–0.28 mM for the immobilization of GOD on colloidal gold modified carbon paste electrode (Liu and Ju, 2003), 0.5–11.1 mM for GOD at a CdS nanoparticles modified electrode (Huang et al., 2005), 0.01–5.5 mM for GOD immobilized on highly ordered polyaniline nanotubes (Wang et al., 2009a,b). The sensitivity of this biosensor is comparable to that of GOD-CNTs-PPF/Au (42 $\mu A\,mM^{-1}\,cm^{-2}$) (Muguruma et al., 2008) and is also much higher than those previously reported, for example, on Nafion-CNTs-CdTe-GOD/GC (14.41 $\mu A\,mM^{-1}\,cm^{-2}$) (Liu et al., 2007), GOD-CNTs-chitosan/GC (7.36 $\mu A\,mM^{-1}\,cm^{-2}$) (Liu et al., 2005) and the CNTs-based multi-layer biosensor (5.6 $\mu A\,mM^{-1}\,cm^{-2}$) (Yan et al., 2007). The detection limit of the biosensor was estimated to be 0.02 mM at a signal-to-noise ratio of 3. The apparent Michealis–Menten constant (K_m^{app}) was also estimated to be 4.4 mM using the Lineweaver–Burk equation (Kang et al., 2007). The result is much smaller than those obtained from GOD-CdS (5.1 mM) (Huang et al., 2005) and Nafion-GOD-SWCNTs (8.5 mM) (Liu et al., 2008b) modified substrate. The reproducibility of the biosensor was investigated using 5.0 mM glucose. With a series of 6 experiments, the relative standard deviation (R.S.D.) of 5.3% was achieved. These results indicated that the immobilized GOD possesses high enzymatic activity, and the graphene–chitosan film provides favorable microenvironment for GOD to perform DET at the modified electrode.

4. Conclusion

We have studied the electrochemical behavior of GOD at a graphene–chitosan modified electrode and demonstrated the direct electron transfer reaction of GOD at the modified electrode. The results indicate that the graphene can provide a favorable microenvironment for the enzyme and promote the direct electron transfer at the electrode surface. Chitosan also plays an important role in forming a well-dispersed graphene suspension and immobilizing the enzyme molecules. This graphene-based enzyme sensor exhibits excellent sensitivity and long-term stability for measuring glucose. The graphene-polymer nanocomposite developed here may offer a new approach for developing novel types of highly sensitive and stable electrochemical biosensors.

Acknowledgments

This work was supported by a laboratory-directed research and development program (LDRD) at Pacific Northwest National Laboratory (PNNL). The work was performed at the Environmental Molecular Sciences Laboratory, a national scientific user facility sponsored by the U.S. Department of Energy (DOE) and located at PNNL. PNNL is operated by Battelle for DOE under Contract DE-AC05-76RL01830. IAA acknowledges support from ARO/MURI under grant number W911NF-04-1-0170.

References

Andreu, R., Ferapontova, E.E., Gorton, L., Calvente, J.J., 2007. J. Phys. Chem. B 111, 469–477.
Ang, P.K., Chen, W., Wee, A.T.S., Loh, K.P., 2008. J. Am. Chem. Soc. 130, 14392–14393.
Ao, Z.M., Yang, J., Li, S., Jiang, Q., 2008. Chem. Phys. Lett. 461, 276–279.
Cai, C.X., Chen, J., 2004. Anal. Biochem. 332, 75–83.
Dai, Z.H., Ni, J., Huang, X.H., Lu, G.F., Bao, J.C., 2007. Bioelectrochemistry 70, 250–256.
Deng, C., Chen, J.H., Chen, X.L., Xiao, C.H., Nie, L.H., Yao, S.Z., 2008. Biosens. Bioelectron. 23, 1272–1277.
Eda, G., Chhowalla, M., 2009. Nano Lett. 9, 814–818.
Ehret, R., Baumann, W., Brischwein, M., Schwinde, A., Stegbauer, K., Wolf, B., 1997. Biosens. Bioelectron. 12, 29–41.
Geim, A.K., Novoselov, K.S., 2007. Nat. Mater. 3, 183–191.
Gooding, J.J., Wibowo, R., Liu, J., Yang, W., Losic, D., Orbons, S., Mearns, F.J., Shapter, J.G., Hibbert, D.B., 2003. J. Am. Chem. Soc. 125, 9006–9007.
Guiseppi-Elie, A., Lei, C., Baughman, R.H., 2002. Nanotechnology 13, 559–564.
Huang, Y.X., Zhang, W.J., Xiao, H., Li, G.X., 2005. Biosens. Bioelectron. 21, 817–821.
Ianniello, R.M., Lindsay, T.J., Yacynych, A.M., 1982. Anal. Chem. 54, 1098–1101.
Jia, J., Wang, B., Wu, A., Cheng, G., Li, Z., Dong, S., 2002. Anal. Chem. 74, 2217–2223.
Kang, X.H., Mai, Z.B., Zou, X.Y., Cai, P.X., Mo, J.Y., 2007. J. Nanosci. Nanotechnol. 7, 1618–1624.
Laviron, E., 1979. J. Electroanal. Chem. 101, 19–28.
Leenaerts, O., Partoens, B., Peeters, F.M., 2008. Phys. Rev. B 77, 125416–125421.
Li, X.L., Wang, X.R., Zhang, L., Lee, S., Dai, H.J., 2008. Science 319, 1229–1232.
Li, D., Kaner, R.B., 2008. Science 320, 1170–1171.
Liu, Q., Lu, X., Li, J., Yao, X., Li, J.H., 2007. Biosens. Bioelectron. 22, 3203–3209.
Liu, B.N., Luo, F., Wu, H.X., Liu, Y.H., Zhang, C., Chen, J., 2008a. Adv. Funct. Mater. 18, 1518–1525.
Liu, S., Ju, H., 2003. Biosens. Bioelectron. 19, 177–183.
Liu, Y., Wang, M.K., Zhao, F., Xu, Z.A., Dong, S.J., 2005. Biosens. Bioelectron. 21, 984–988.
Liu, X.Q., Shi, L.H., Niu, W.X., Li, H.J., Xu, G.B., 2008b. Biosens. Bioelectron. 23, 1887–1890.
Luo, X., Killard, A.J., Smyth, M.R., 2006. Electroanalysis 18, 1131–1134.
McAllister, M.J., Li, J.L., Adamson, D.H., Schniepp, H.C., Abdala, A.A., Liu, J., Herrera-Alonso, M., Milius, D.L., Car, R., Prud'homme, R.K., Aksay, I.A., 2007. Chem. Mater. 19, 4396–4404.
Muguruma, H., Shibayama, Y., Matsui, Y., 2008. Biosens. Bioelectron. 23, 827–832.
Nadzhafova, O., Etienne, M., Walcarius, A., 2007. Electrochem. Commun. 9, 1189–1195.
Niyogi, S., Bekyarova, E., Itkis, M.E., Mcwilliams, J.L., Hamon, M.A., Haddon, R.C., 2006. J. Am. Chem. Soc. 128, 7720–7721.
Novoselov, K.S., Geim, A.K., Morozov, S.V., Jiang, D., Zhang, Y., Dubonos, S.V., Grigorieva, I.V., Firsov, A.A., 2004. Science 306, 666–669.
Peres, N.M.R., Guinea, F., Castro Neto, A.H., 2006. Phys. Rev. B 73, 125411–125423.
Pulcu, G.S., Elmore, B.L., Arciero, D.M., Hooper, A.B., Elliott, S.J., 2007. J. Am. Chem. Soc. 129, 1838–1839.
Schedin, F., Geim, A.K., Morozov, S.V., Hill, E.W., Blake, P., Katsnelson, M.I., Novosenlov, K.S., 2007. Nat. Mater. 6, 652–655.
Schniepp, H.C., Li, J.L., Mcallister, M.J., Sai, H., Herrera-Alonso, M., Adamson, D.H., Prud'homme, R.K., Car, R., Saville, D.A., Aksay, I.A., 2006. J. Phys. Chem. B 110, 8535–8539.
Shan, D., Wang, S., Xue, H., Cosnier, S., 2007. Electrochem. Commun. 9, 529–534.
Shan, C.S., Yang, H.F., Song, J.F., Han, D.X., Ivaska, A., Niu, L., 2009. Anal. Chem. 81, 2378–2382.
Stankovich, S., Dikin, D.A., Dommett, G.H.B., Kohlhaas, K.M., Zimney, E.J., Stach, E.A., Piner, R.D., Nguyen, S.T., Ruoff, R.S., 2006. Nature 442, 282–286.
Vivekchand, S.R.C., Rout, C.S., Subrahmanyam, K.S., Govindaraj, A., Rao, C.N.R.J., 2008. J. Chem. Sci. 120, 9–13.
Wang, J., Li, M., Shi, Z., Li, N., Gu, Z., 2002. Anal. Chem. 74, 1993–1997.
Wang, X., Zhi, L.J., Mullen, K., 2008. Nano Lett. 8, 323–327.
Wang, Y., Li, Y.M., Tang, L.H., Lu, J., Li, J.H., 2009a. Electrochem. Commun. 11, 889–892.
Wang, Z., Liu, S.N., Wu, P., Cai, C.X., 2009b. Anal. Chem. 81, 1638–1645.
Wen, D., Liu, Y., Yang, G.C., Dong, S.J., 2007. Electrochim. Acta 52, 5312–5317.
Xu, C., Wang, X., Zhu, J.W., 2008a. J. Phys. Chem. C 112, 19841–19845.
Xu, Y., Bai, H., Lu, G.W., Li, C., Shi, G.Q., 2008b. J. Am. Chem. Soc. 130, 5856–5857.
Yan, X.B., Chen, X.J., Tay, B.K., Khor, K.A., 2007. Electrochem. Commun. 9, 1269–1275.
Yi, H.M., Wu, L.Q., Bentley, W.E., Ghodssi, R., Rubloff, G.W., Culver, J.N., Payne, G.F., 2005. Biomacromolecules 6, 2881–2894.
Zhang, L., Zhang, Q., Li, J.H., 2007. Electrochem. Commun. 9, 1530–1535.
Zhang, M.G., Smith, A., Gorski, W., 2004. Anal. Chem. 76, 5045–5050.
Zhao, X.J., Mai, Z.B., Kang, X.H., Zou, X.Y., 2008a. Biosens. Bioelectron. 23, 1032–1038.
Zhao, X.J., Mai, Z.B., Kang, X.H., Dai, Z., Zou, X.Y., 2008b. Electrochim. Acta 53, 4732–4739.
Zhou, Y., Yang, H., Chen, H.Y., 2008. Talanta 76, 419–423.